

Implicit modelling workflow for a geotechnical model for rapid integration and its calibration for application at Tropicana gold mine

Joao Ramires ^{a,*}, Damian Reardon ^b, Kayla Gosche ^a

^a AngloGold Ashanti, Australia

^b Dynamic Geotechs, Australia

Abstract

Spatial modelling of geotechnical variables is vital to guide mine designs by highlighting risks and opportunities in advance. Specifically for open stope underground mines, the modelling of the rock mass quality using Q' (Potvin 1988) and uniaxial compressive strength (UCS) allows the estimation of stable stope spans and minimum pillar requirements. The resulting extraction ratios (ER%) are loaded into the geotechnical model for rapid integration (GMRi) and provided to mine planners before design of the stoping areas. This process has been successfully semi-automated at Tropicana gold mine (TGM) in Australia by AngloGold Ashanti (AGA). The current rock mass modelling methodology uses implicit links to combine the geological model and geotechnical datasets in a single modelling project. This paper aims to present an implicit modelling workflow to update the GMRi and the application of this process at TGM to allow forecasting of declining extraction ratios at depth many years in advance, providing the opportunity for the business to proactively consider alternative mining methods.

Keywords: *implicit modelling, extraction ratio, rock mass modelling, geotechnical model for rapid integration*

1 Introduction

Tropicana gold mine (TGM) is located 330 km northeast of Kalgoorlie and 200 km east of Laverton, Western Australia. It produces gold-bearing ore from several open pits and from underground. The open pits are named, from north to south: Boston Shaker, Tropicana, Havana and Havana South. The underground mine is located beneath the Boston Shaker and Tropicana open pits. The orebodies mined underground are typically shallow dipping (23–47°) (Figure 1) and have been in production since August 2020. Mining is via pillars and longhole open stoping methods and, due to favourable current stress levels, backfill methods for stope voids are currently not used, with most stope voids remaining open for the life of mine.

The shallow-dipping stopes (on average, 17.5 m high, 30 m strike and 35 m dip) employ cable bolts (Figure 2) as pattern anchor support along overlapping stope spans to limit large connecting spans, and to assist with regional stability and reduce dilution locally.

The expansion and ramp up of underground operations at TGM remain a focus for mine planning, geology and geotechnical teams, as shown in Figure 3. Several underground mining trade-off strategies are assessed as part of yearly strategy and budget cycles, including varying cut-off grades' (COG) scenarios and stoping thicknesses. The underground mining scenarios result in variable stoping thicknesses. This results in changes to pillar strike dimensions to maintain stable width to height ratios (W:H) (Lunder & Pakalnis 1991), ultimately impacting extraction ratios (ER%). In these scenarios, reductions in COG do not necessarily yield increased ore tonnes or recovered ounces for the business (Figure 4). For example, a W:H ratio of 0.5 would yield a typical pillar strike length of 7.5 m for a 3 g/t Mineable Shape Optimizer (MSO) option, whereas bulking the

* Corresponding author. Email address: joao.fochi@gmail.com

orebody out to a 1.5 g/t MSO COG option would require a typical pillar strike length of 15 m for the same mining area, resulting in a lower extraction ratio for each mining level.

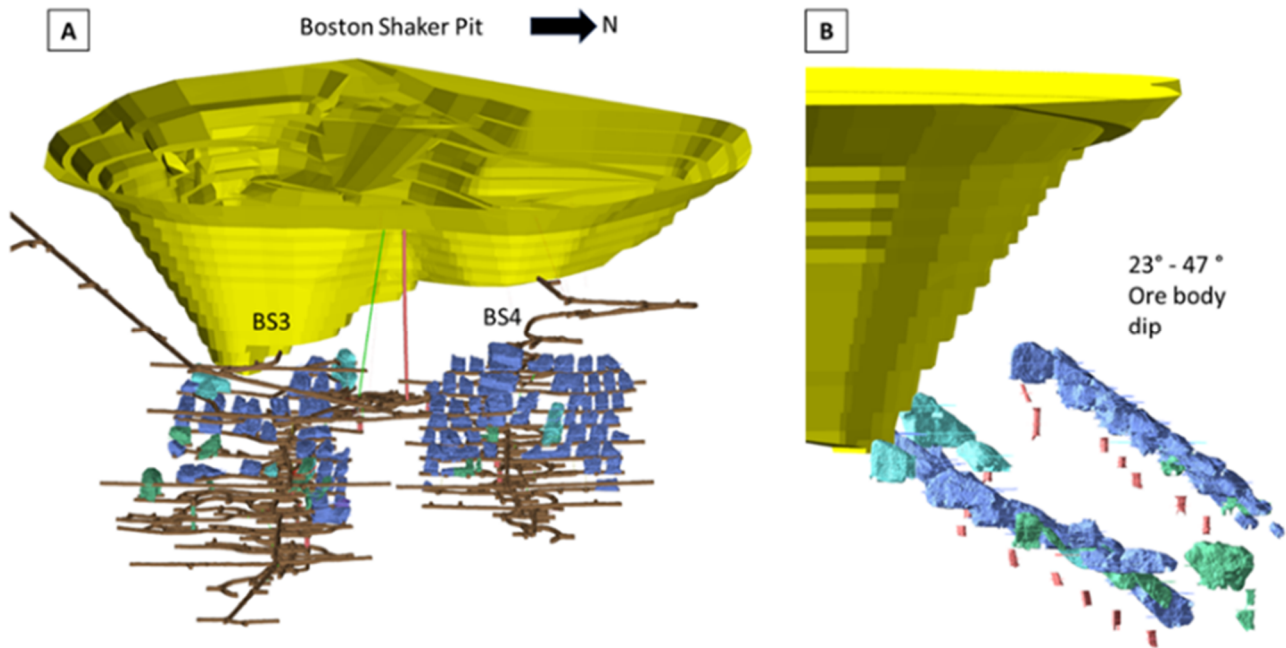


Figure 1 Overview of Boston Shaker underground mine: (a) Looking west showing the pit, Boston Shaker 3 and Boston Shaker 4 mining areas with mined drives and stope voids; (b) View looking north showing the shallow dip of the Boston Shaker orebody (Fernandes et al. 2024)

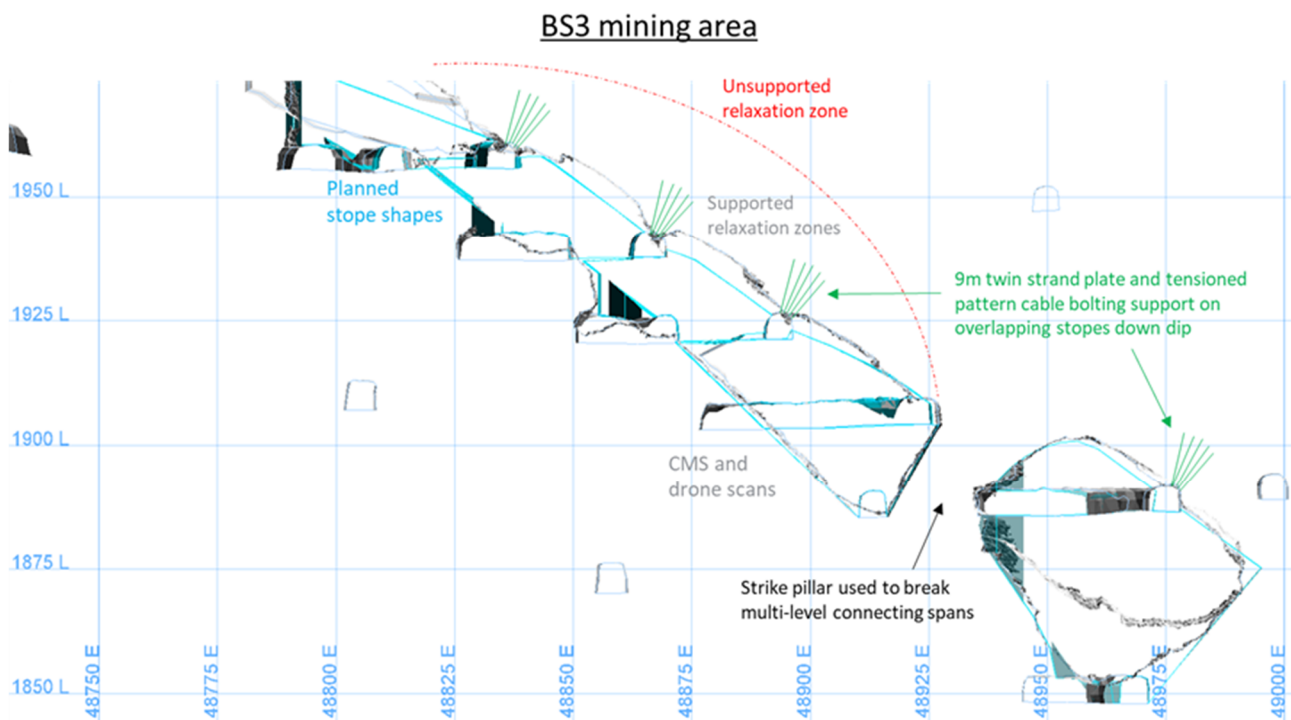


Figure 2 Cross-sectional view looking north, showing pattern 9 m double strand cable bolting support creating a supported rock beam to limit the down-dip span (Fernandes et al. 2024)

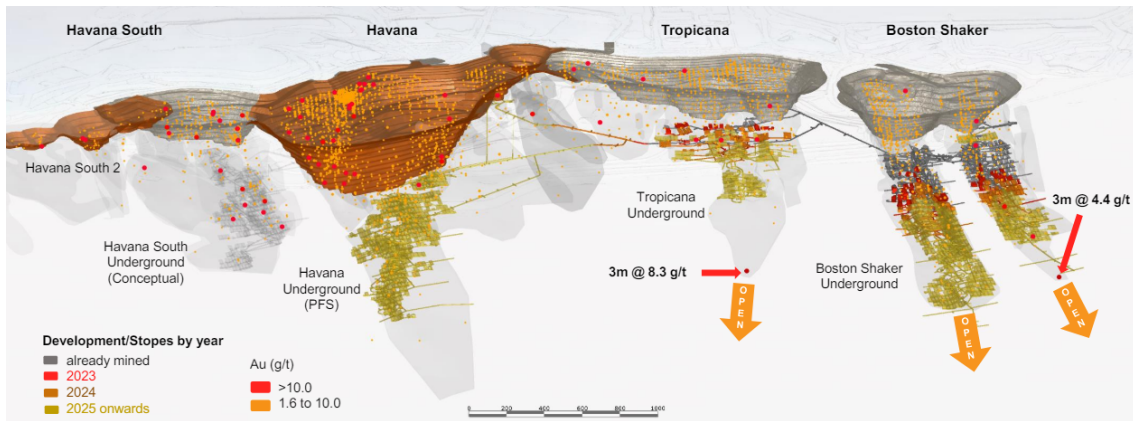


Figure 3 Tropicana gold mine overview (Briggs 2023)

Uniaxial compressive strength (UCS) values (from Equotip measurements of core) (Banff 2018), and Q' data from diamond core and scanline mapping, are used in the rock mass model (RMM). ER% estimations (Figure 5) are calculated in the site's geotechnical model for rapid integration (GMRI) (Hamman et al. 2017), incorporating site-specific stability criteria and equivalent linear overbreak sloughage (ELOS) curves (Fernandes et al. 2024), and the site's most recent in situ over-core stress measurements.

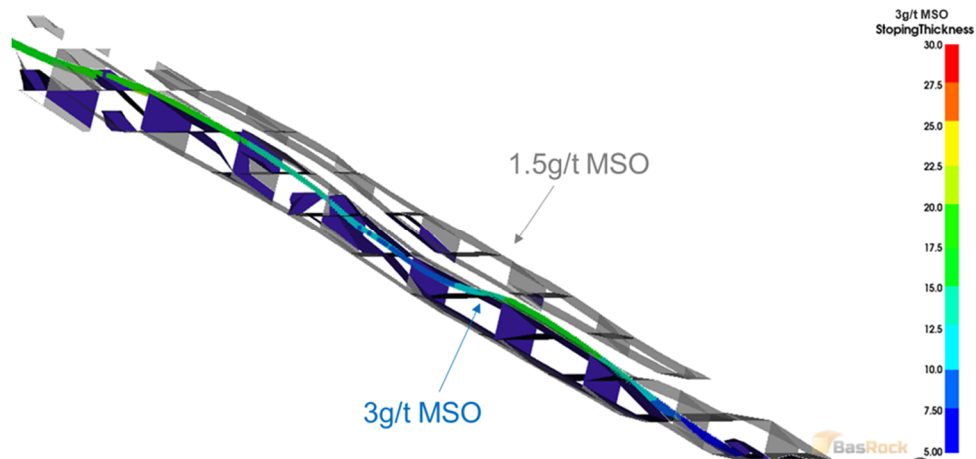


Figure 4 Variance in mineable shape optimiser stopes for varying cut-off grades, impacting stoping thickness and, in turn, extraction ratios

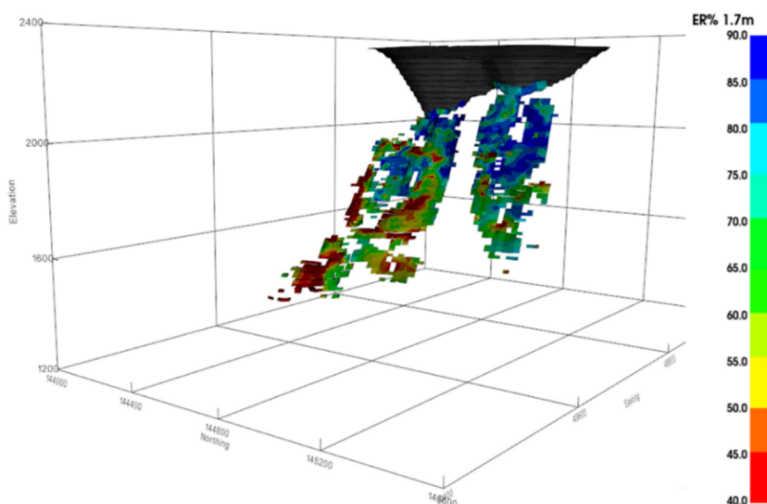


Figure 5 Extraction ratios for a 1.7 m equivalent linear overbreak sloughage stoping option, colour-coded to stoping areas for a typical business cut-off grade scenario

Therefore, to streamline the modelling flow and ensure consistency in geotechnical assessments, a semi-automated modelling process via implicit modelling was developed to ensure the most up-to-date geotechnical information is available to support the business in making effective decisions on varying COG scenarios and schedules.

2 Methodology

The TGM RMM implicit methodology uses two sources of information. It combines a stoping-specific Q' named Q_s' (Fernandes et al. 2024) and UCS datasets with the geological model domains. The Q_s' and UCS datasets are transferred to the RMM through comma-separated values (.csv) from GeotAgg, while the geological model is updated seamlessly through Leapfrog Central links (Seequent 2024).

By using the Leapfrog Edge extension (Seequent 2024), the shapes of geology domains and the values of Q_s' and UCS are integrated for spatial analysis (variography). Numeric estimations are performed using decluttered Q_s' and UCS values via inverse distance squared weighted (IDW^2) estimator (Isaaks & Srivastava 1989). Each IDW^2 estimation is restricted to its respective geology domain boundaries and fitted to its variogram model. Despite IDW^2 being a global estimator, in this process the IDW^2 is fitted to a variogram model to determine Q_s' spatial autocorrelation for each domain and to manage the levels of confidence within the estimated model results. Additionally, to ensure IDW^2 provides good adherence to the data, the IDW^2 results are back-flagged to the data points and cross-validated to reach a strong correlation factor ($R^2 \geq 95$) for each domain.

The orebody models are also shared via Leapfrog Central, which enables the separation of hanging wall (HW) and footwall (FW) wireframes as distinct surfaces. These surfaces can be smoothed using GEM4D software (Basson 2024) to estimate the stoping thickness (the distance between the FW of the orebody and the HW of the orebody). The stress model is completed in Map3D (Wiles 2023) using a range of typical pillar orientations, and the results are transferred to the GMRi Excel file via Macro link. This allows stress level estimations to be included in stope and pillar designs relative to the orebody's UCS.

Figure 6 shows the TGM modelling process flow employed to support business decision-making. It ensures the use of up-to-date geotechnical information in different COG scenarios and schedules.

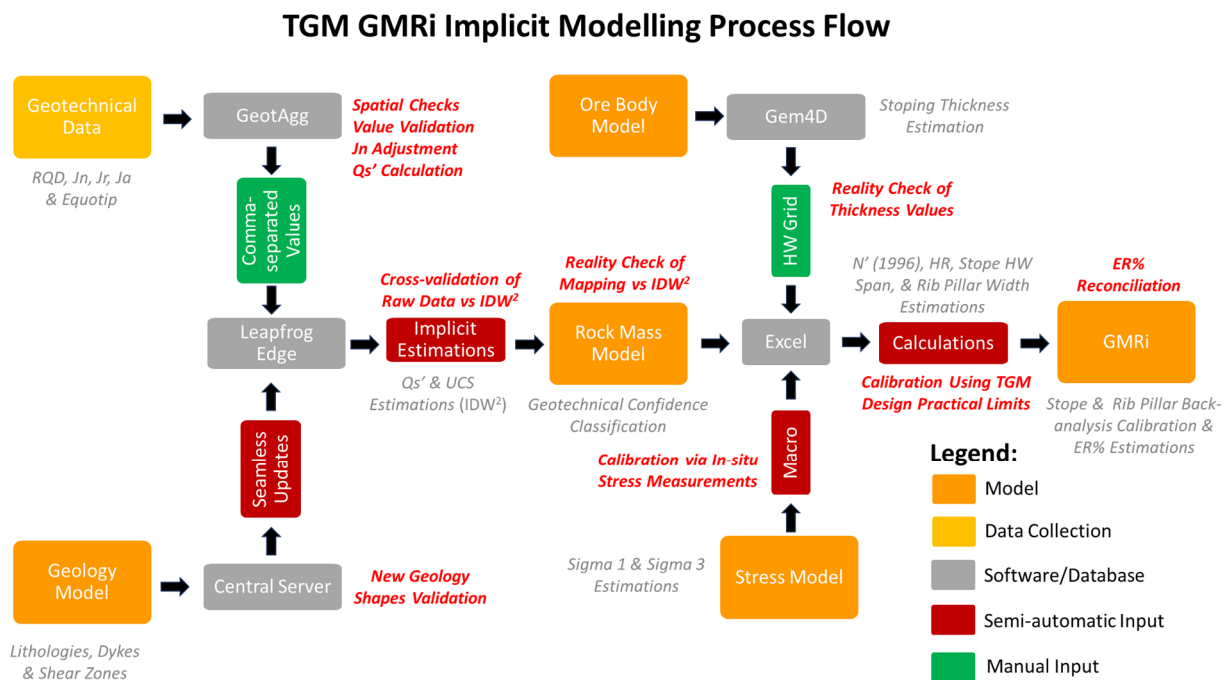


Figure 6 Tropicana gold mine geotechnical streamlined implicit modelling process flow

2.1 Geotechnical data processes

TGM geotechnical data is secured in the AGA centralised group database (GeotAgg) (Hamman et al. 2017). This allows access to standardised processing, calculations and subsequent tools, features and reports.

2.1.1 GeotAgg data exports

GeotAgg exports are imported for use in the Leapfrog project. This provides updated data to the RMM frequently, ensuring the data is readily available. These exports are in .csv format and at a set location on the TGM file server. There are two data tables currently exported from GeotAgg. They are the combined Q' data from logging and mapping and the Equotip data. Adjustments, checks and calculations are completed on the data automatically before exporting to Excel. These allow the data to be ready for import to the model and are outlined in Sections 2.1.2 to 2.1.5.

2.1.2 Data quality checks

Data quality checks performed in GeotAgg enable the exports to have improved functionality when importing to the Leapfrog project. Two types of checks are performed: spatial checks (do we have the data available to view this point in space, such as collar and surveys and sequential intervals) and value validation checks (are the logged/mapped values within our expected ranges). Data is validated and exported spatially to ensure consistency between geology units.

2.1.3 Logging data adjustments

Comparisons of mapping and logging Q' datasets show if a bias is apparent. The joint set number (J_n) (Norwegian Geotechnical Institute 2015) parameter is directionally controlled and a primary source of error. Figure 7 shows this bias with a spatial comparison of mapping and logging values. J_n values are higher (indicating more sets) from mapping than the values visually logged from the core. As mapping data considers a larger exposure in 3D, J_n adjustments were introduced to match the drilling data to the mapping data. These adjustments were built into the export file for use in the RMM.

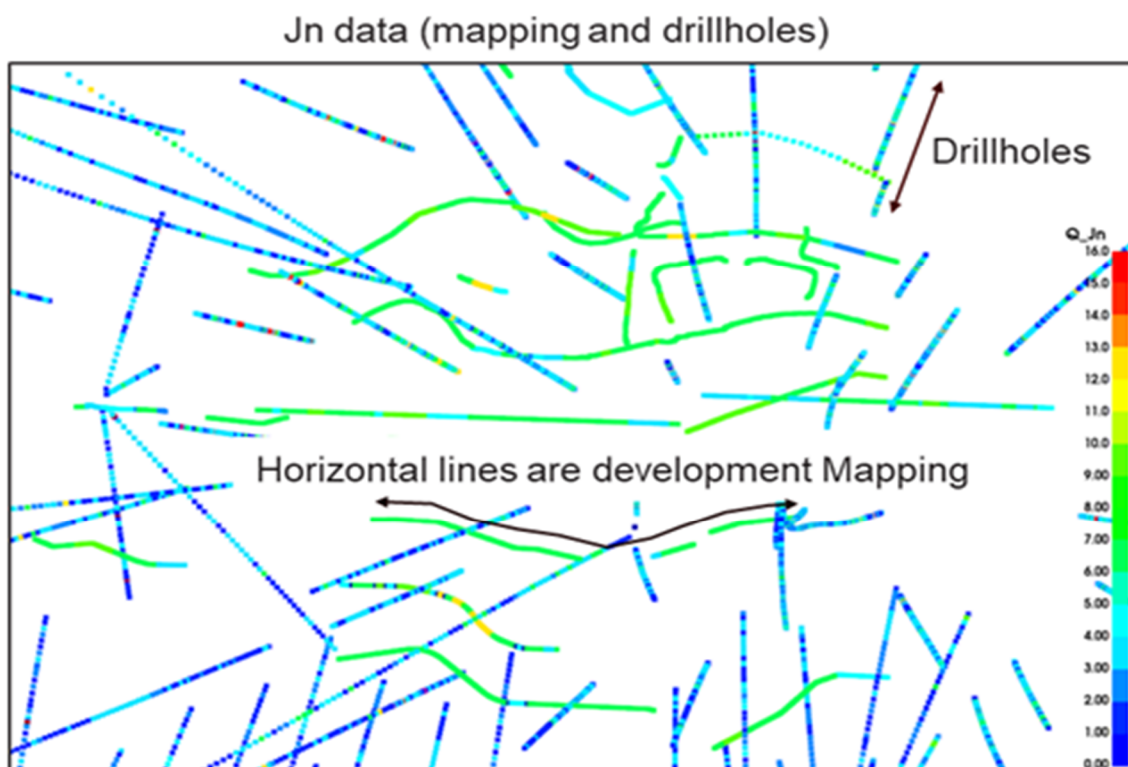


Figure 7 Directional bias observed in the logging joint set number parameter

Figure 8 shows the Jn adjustments applied to the logging data for each lithological domain and the resulting correlation to the mapping values (Reardon 2023).

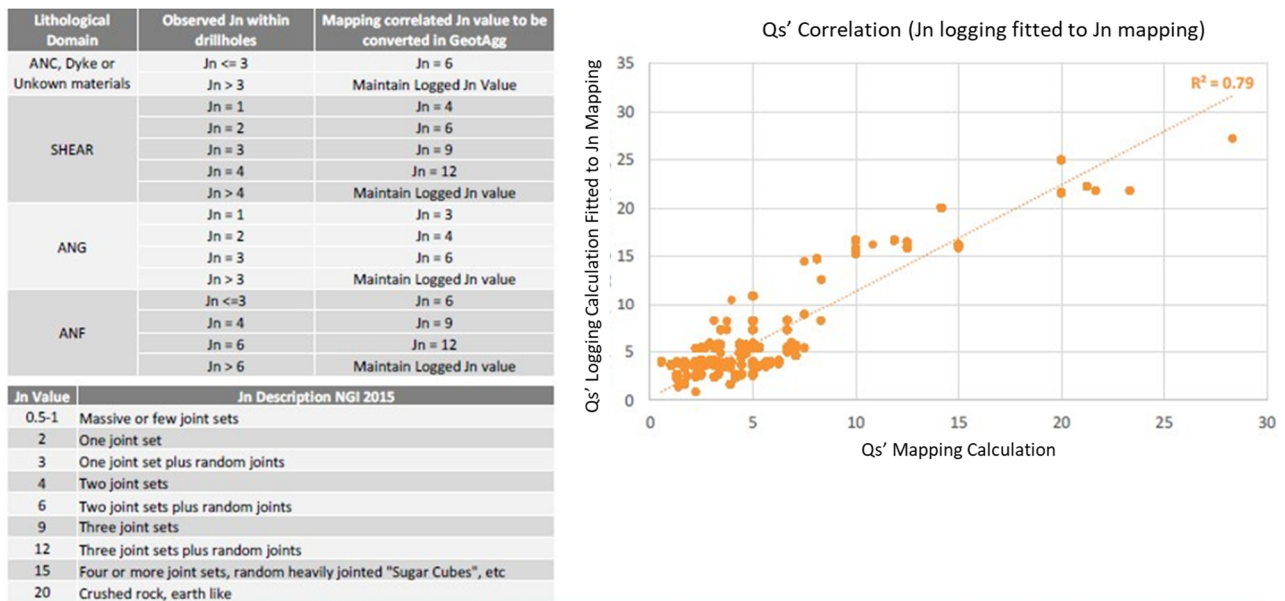


Figure 8 Joint set number correlation employed to fit joint set number logging classes to joint set number mapping underground to adjust the directional control bias

2.1.4 Stoping Q' calculation

A stoping-specific Q' (Qs') was developed for TGM due to the flat dipping nature of the orebody (Fernandes et al. 2024) and integrated into the .csv export file. Early stoping back-analysis revealed that joint roughness (Jr) had a negligible impact on stope stability due to the joints acting in tension and no sliding contributing to HW overbreak. This led to incorporating a site-specific Qs' formula (Equation 1) into stope assessments.

$$Qs' = \frac{RQD}{Jn} \times \frac{1}{Ja} \tag{1}$$

This has flowed on to improvements in predicting actual stope behaviour at the mine, allowing the business to maximise the ER% without the negative effects of large stope overbreak and dilution.

2.1.5 Equotip correlation to uniaxial compressive strength

TGM has extensive Equotip readings, available from drillcore measurements, using a Leeb hardness impact device Type D (HLD) typically completed every 3 m. These have been converted to UCS for use in the RMM via the .csv file. Equation 2 shows the UCS/HLD correlation developed for TGM, while Figure 9 shows the relationship between UCS and HLD (Banff 2018).

$$UCS = 1.4048e^{0.0059*HLD} \tag{2}$$

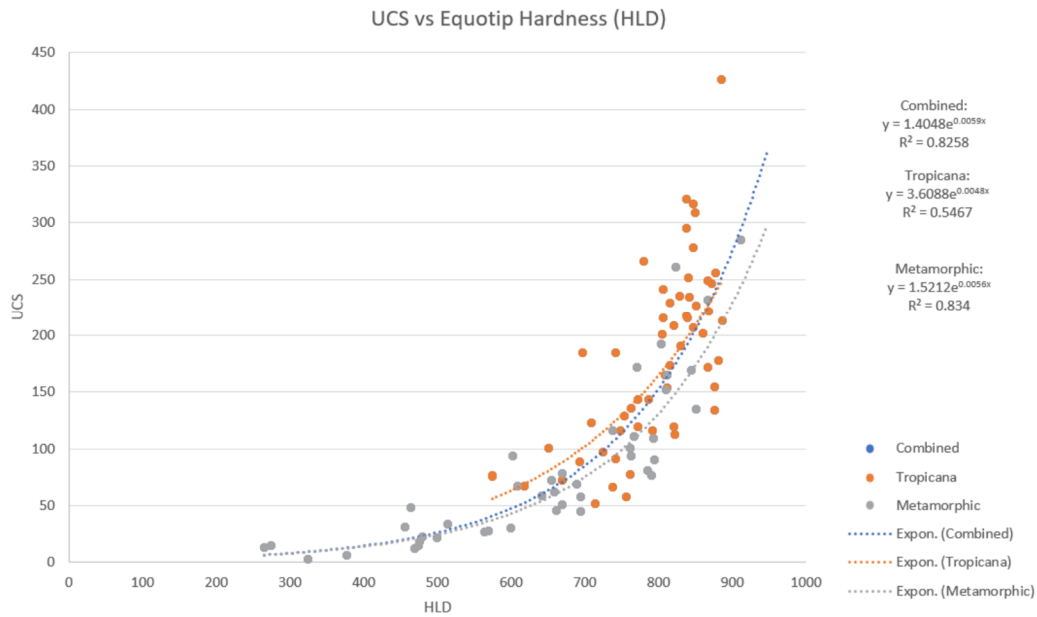


Figure 9 Curve fitted to Equotip data collected at Tropicana gold mine and other sources from literature (Banff 2018)

2.2 Geological model links via central

The TGM geology department regularly updates the geological models to facilitate the strategic planning cycle. Lithologies, alterations and large structure models are included in these updates. These support the modelling of orebodies, which provides the basis for resource estimation and, ultimately, the mine plan and design. Likewise, using the geological model domains in the RMM is essential to ensure accurate estimations of rock mass variables. The geological model shapes serve as a boundary for numeric estimations and ensure that the data from the same domain with similar mechanical and spatial behaviours are spatially correlated. This correlation is crucial in providing reliable estimations of Q_s' and UCS (Figure 10).

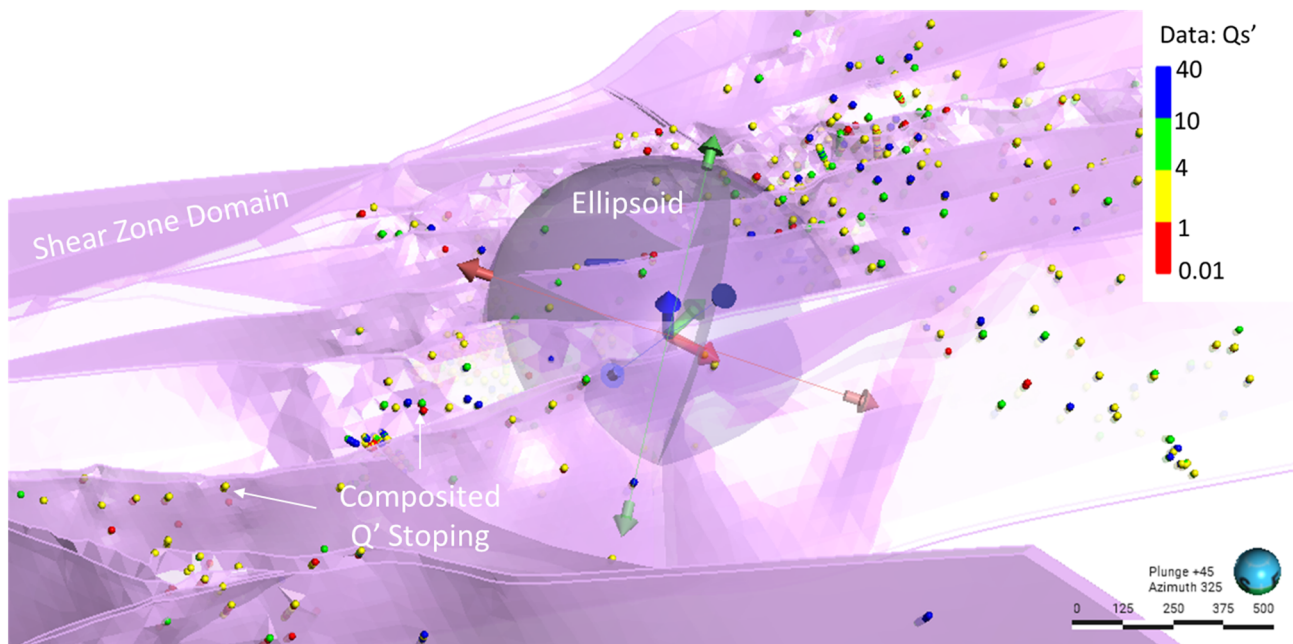


Figure 10 Q_s' spatial analysis inside the shear zone domain as an example of the domained estimation function employed

TGM geological models have been integrated into the RMM Leapfrog project using Central Solutions from Seequent. This integration ensures the latest geological information is available when modelling Q_s' and UCS datasets. Leapfrog Central technologies increase productivity by allowing for seamless updates between different modelling projects (Seequent 2024).

2.3 Implicit block estimation

The process of numerical estimation is conducted separately for the Q_s' and UCS data. Each estimation is performed per geological domain, such as a shear zone or garnet gneiss unit. For example, in Figure 10 the Q_s' estimation is done only for Q_s' values within the shear zone shape. The goal is to avoid mixing different datasets that may be spatially correlated and create unrealistic rock mass conditions.

Figure 10 also showcases the Edge's domained estimation function, which integrates geology domains and numeric variables for spatial analysis. The domains and variables are connected via implicit links to enable seamless updates (Seequent 2024).

To begin the spatial modelling process the data within the specific domain is first normalised. Figure 11 displays the normalised Q_s' histogram and the Hermite fit used to validate the normalisation. The next step involves analysing the longest spatial autocorrelation orientation of the variable within the domain boundary, as illustrated in Figure 12.

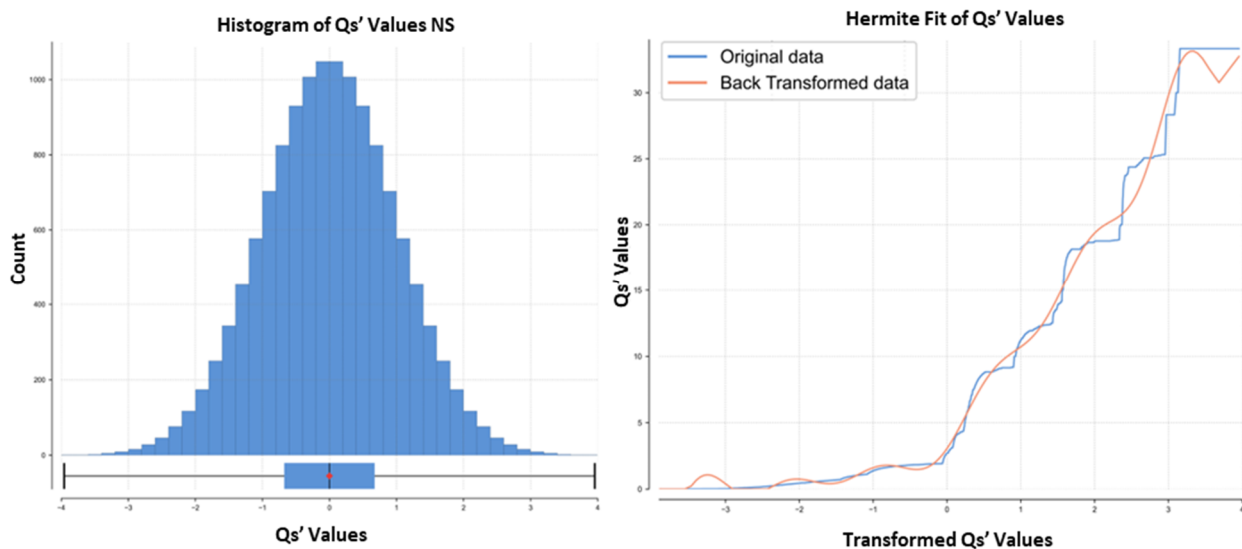


Figure 11 Q_s' normalised histogram on the left and Hermite fit validation on the right

After determining the variable preferential orientation the analysis proceeds as shown in Figure 12. This involves testing various potential variogram models (line) and identifying the best fit for the experimental variogram (points). In this process it considers the three ellipsoid axes: major (red), semi-major (green) and minor (blue).

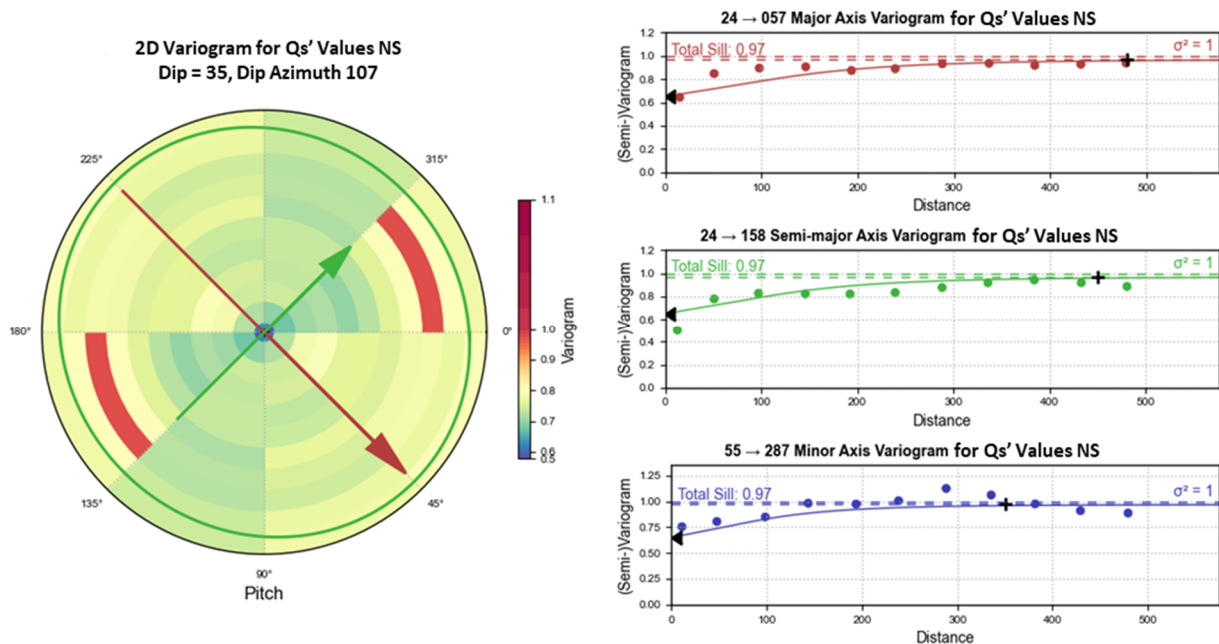


Figure 12 Example of variographic analysis performed for Q' stopping inside the shear zone domain

The selected variogram model is used to create a spatial trend with variable orientation. This process combines the properties of the variogram, such as dip, azimuth, pitch, and major, semi-major and minor axes, with the contact surfaces of the domain. This structural trend then drives the numeric estimation throughout the domain space, taking into consideration its morphological variations. See Figure 13 for a visual representation.

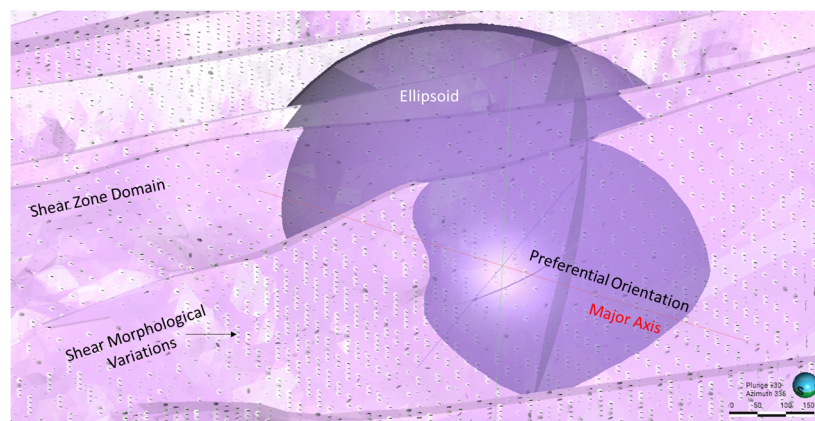


Figure 13 Example of trend variable orientation constructed to drive Qs' across the shear zone morphological variations

Before estimating the model the data is declustered within each domain using its variogram results. Figure 14 demonstrates shear zone domain Qs' values declusterisation using the variogram results. After completing the analysis using the steps outlined above, the estimation of Qs' is done using IDW² for each domain individually. Every estimation takes into consideration the declustered data and its particular variogram and trend. Figure 15 showcases a visual example of Qs' stopping IDW² results for the shear zone domain. The IDW² has been used to evaluate the shear zone wireframe vertices, providing visual validation of the results.

To ensure that the model accurately reflects the data, a cross-validation between the Qs' raw values and the Qs' IDW² results is conducted on Leapfrog Edge. The raw data points are marked with the IDW² results and then a linear regression is performed to compare the raw data against the IDW² for each domain. Finally, each estimation is refined until a strong correlation is achieved ($R^2 \geq 0.95$), as shown in Figure 16, to ensure the data is honoured to the greatest extent possible.

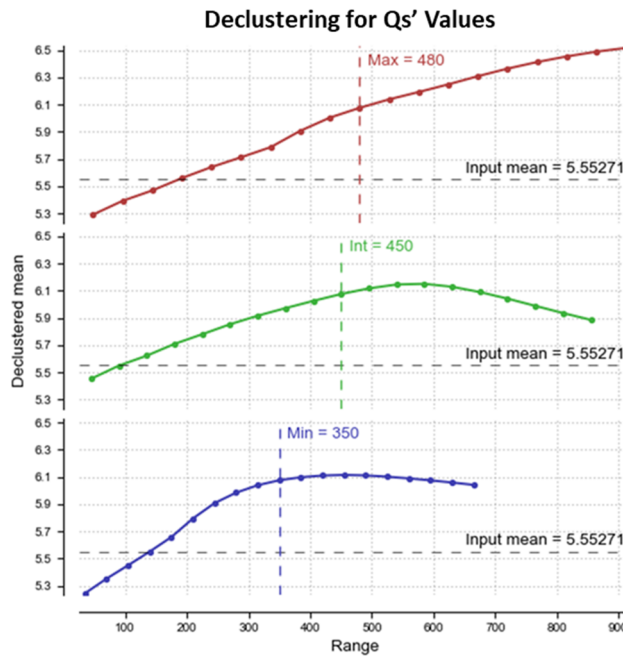


Figure 14 Shear zone domain Qs' declusterisation using the variogram results

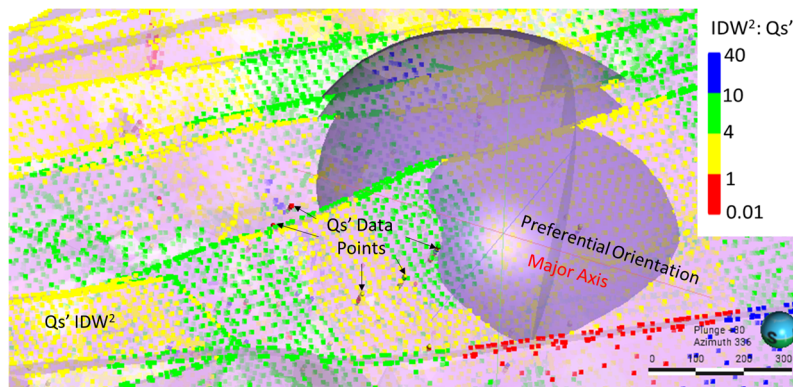


Figure 15 Qs' inverse distance squared weighted results evaluated in the shear surface vertices for visual validation

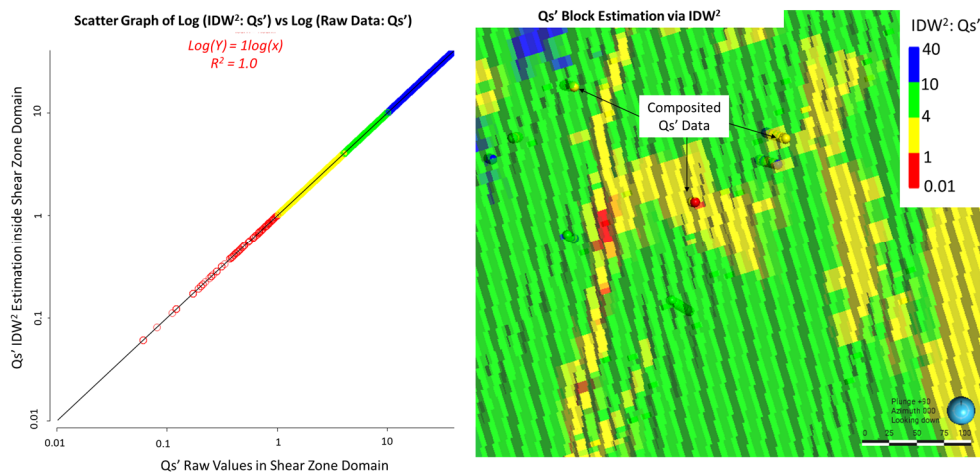


Figure 16 Qs' estimation cross-validation results. The left graph demonstrates the cross-validation results and the model on the right demonstrates the rock mass model block estimation matching the simulated dataset

The individual estimations for each domain are combined into a single estimator that integrates all of them while respecting the chronological order set in the geology model. This combined estimator is then blocked based on the confidence level analysis presented in Figure 17.

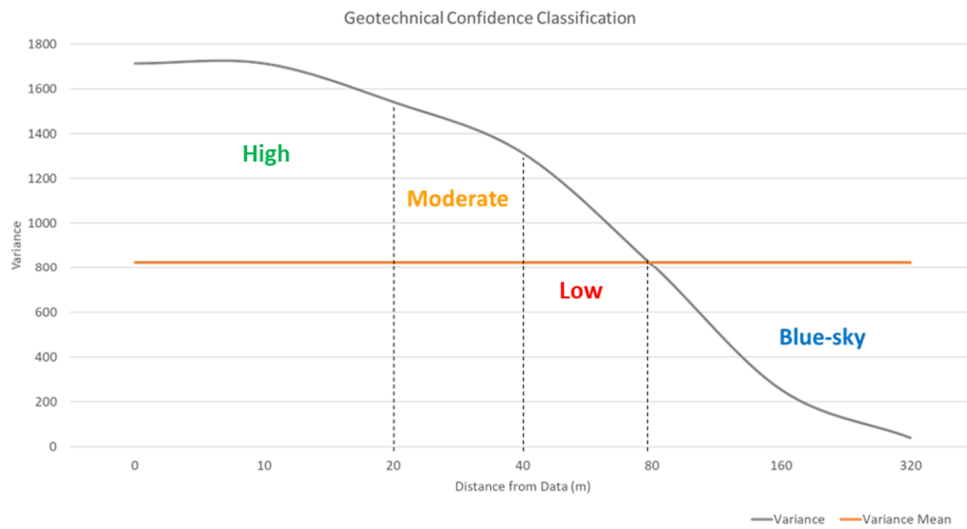


Figure 17 Rock mass model confidence based on the distance from input datasets, i.e. logging and mapping

The blocks are oriented according to the orebody shape to reduce contact distortion bias. The block dimension for the geotechnical model is set at X = 10 m, Y = 20 m and Z = 5 m, capping the X axis at 50% of the distance of the high confidence class inside good lithology domains. However, the model is sub-blocked at X = 5 m, Y = 10 m and Z = 2.5 m inside the poor structure domains to enhance resolution where geotechnical hazards are expected. The model boundary is set to encompass the entire life of mine design, which aims to provide quick updates on estimations.

This process is repeated for UCS data and both combined estimators, i.e. Q_s' and UCS are integrated into the RMM (block model). Figure 18 visually displays the Boston Shaker RMM Q_s' IDW² results, following the methodology described.

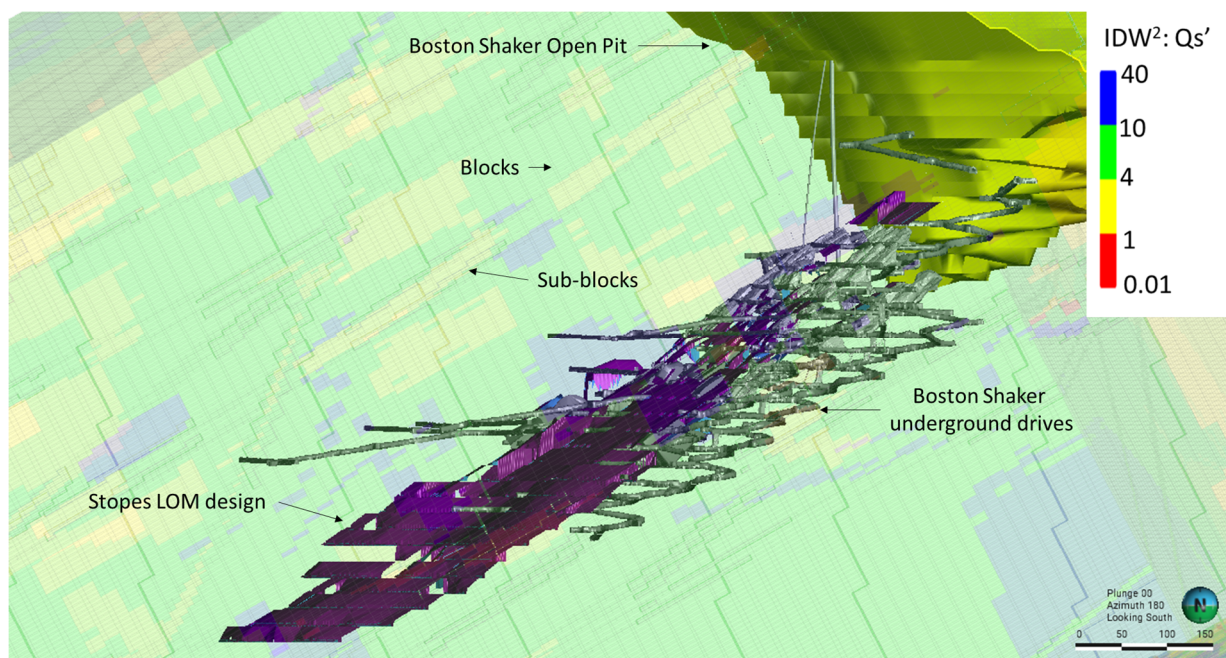


Figure 18 Boston shaker rock mass model looking south and displaying Q_s' inverse distance squared weighted results for the life of mine

2.4 Confidence levels

Figure 17 shows the adopted confidence levels used to address uncertainty in the model. This classification is based on the distance between the estimated data and each block in the model. The variance of the IDW² results across different distance lags is compared to the mean data variance. It is worth noting that the model variance drops below the variance mean when the distance is greater than 80 m from the data. This indicates a Blue sky level of confidence.

The tighter the data grid spacing gets the better the model outcomes are. This is to provide enough resolution and capture all variability within the production design. The confidence classification is integrated into the RMM to manage uncertainty levels. It can also provide guidance for data-collection strategies to enhance data resolution following the annual budget and strategy cycles.

Ideally stope design for the short- to medium-term, over the next two years of production, should be at high confidence levels. This will provide sufficient detail for the GMRi assessment. Long-term stope design (MSO stope shapes) should be at moderate confidence levels. However, the confidence levels are expected to decrease towards the end of the mine’s life. It’s important to note that any Blue sky levels should not be considered in the GMRi assessment.

2.5 Mine design integration

The mine planning team re-runs MSO stopes, mining schedules and COG scenarios on a yearly or half-yearly basis to assess new areas of mineral resources and reserves, and to update costs and gold price assumptions. During this process geotechnical inputs assign an individual ER% to each MSO stope shape, defined by the stope centroid exported from Deswik mining software (Deswik 2024). The ER% for each stope centroid is calculated from the site’s GMRi using the formula below (Equation 3):

$$ER\% = \frac{\text{Stope HW Strike Span}}{\text{Stope HW Strike Span} + \text{Rib Pillar Strike Length}} \times 100 \quad (3)$$

Grade shells are created based on various COG scenarios requested by mine planning in Leapfrog (e.g. 1.5, 2.1, 2.7 and 3 g/t COG scenarios). The HW and FW are then extracted as individual surfaces and smoothed in GEM4D software (Basson 2024).

The HW and FW COG wireframes are checked in 3D to confirm that they mostly align with the proposed MSO shapes from mine planning for HW and FW placement. HW data is extracted from the mesh into .csv format, typically on a 5 or 10 m spacing. Stopping thickness is defined by a distance search option in GEM4D for each HW point searching towards the nearest point of the FW wireframe (Figure 19).

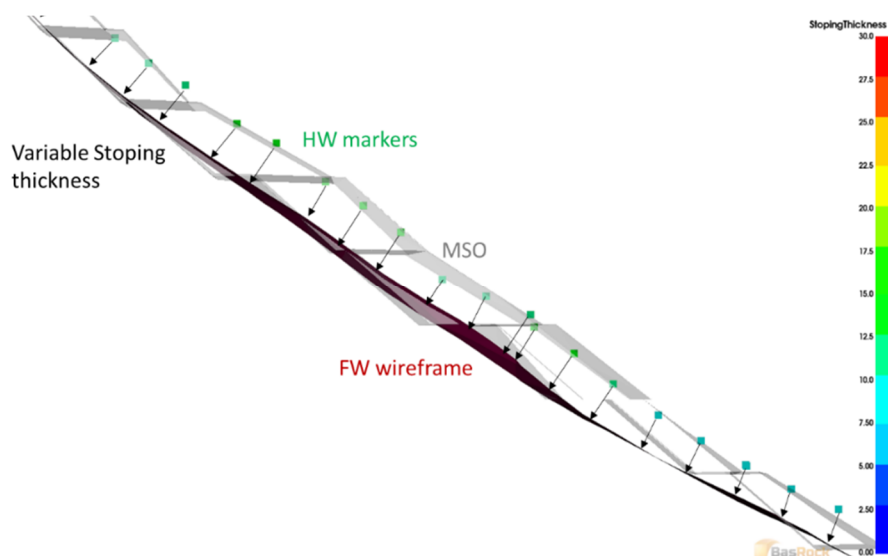


Figure 19 Variable stopping thickness for cut-off grade wireframe calculated from hanging wall marker to footwall wireframe, section view looking north

Geotechnical information from the RMM is applied to the HW markers; in particular, information required to calculate N' for modified Mathews et al. (1981), HW stability by Potvin (1988) and ELOS estimates (Clark & Pakalnis 1997). These assessment methods have been refined by site-specific work (Fernandes et al. 2024) to allow more accurate stoping prediction by plotting N' and Qs' . Geotechnical information suitable for calculating pillar stability based on UCS (calculated from Equotip) is also applied from the RMM to the HW markers.

The final step involves allocating the nearest geotechnical information (including ER%) back to each MSO stope centroid using a Nearest Neighbour interpolator (Isaaks & Srivastava 1989) in GEM4D (Figure 20). These updated mining parameters are then used by the business to forecast ounce delivery and identify areas of risk or opportunity and cash flows.

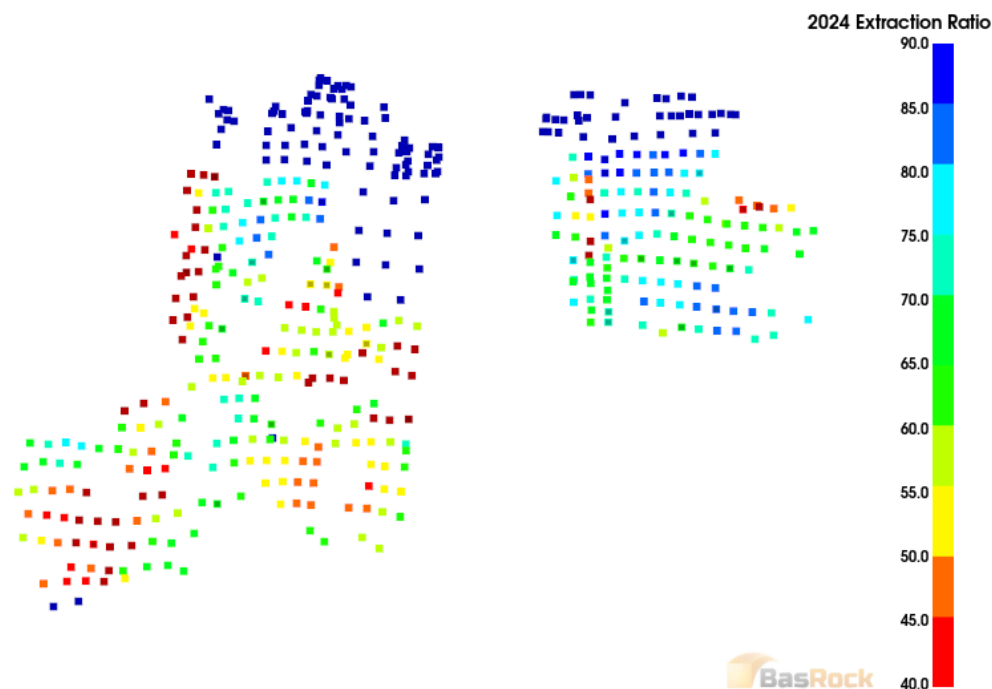


Figure 20 2024 extraction ratios applied to stope centroids in the Deswik schedule (as the schedule includes both approved mining shapes and pillars combined with conceptual Mineable Shape Optimizer shapes, areas above 90% extraction ratio generally have stope notes already completed and pillars designed)

3 Results

The GMRI methodology was implemented in TGM during the underground Boston Shaker feasibility study in 2019 and has been under calibration since then to ensure strong confidence in predicting ER%. Checking areas of predicted ground conditions (core logging Qs' versus observed mapping Q') is particularly important in building confidence and reliability in the RMM. Similarly, another key factor is tracking the stoping and pillar performance and comparing them to the conditions predicted in the GMRI.

3.1 Model reconciliation

The site geotechnical team completes mapping of development drives to validate design assumptions used in ground support and stope note assessments. Figure 21 demonstrates an example of the model validation performed for the RMM using the geotechnical Q' mapping information in BS3 2062 level. Furthermore, Figure 22 demonstrates the field validation results performed for four levels within Boston Shaker (BS3 2062, BS3 2015, BS3 2034, and BS4 2115).

Pillar behaviour and stress levels are key drivers for the ER%. Due to typical pillar dimensions and blast damage observed, a 6 m minimum pillar strike is used in the GMRI, with a minimum W:H ratio of 0.4.

The mine targets a pillar Factor of Safety (FoS) between 1.0 and 1.4, depending on location, risk tolerance and potential impacts to surrounding mining areas (Figure 23).

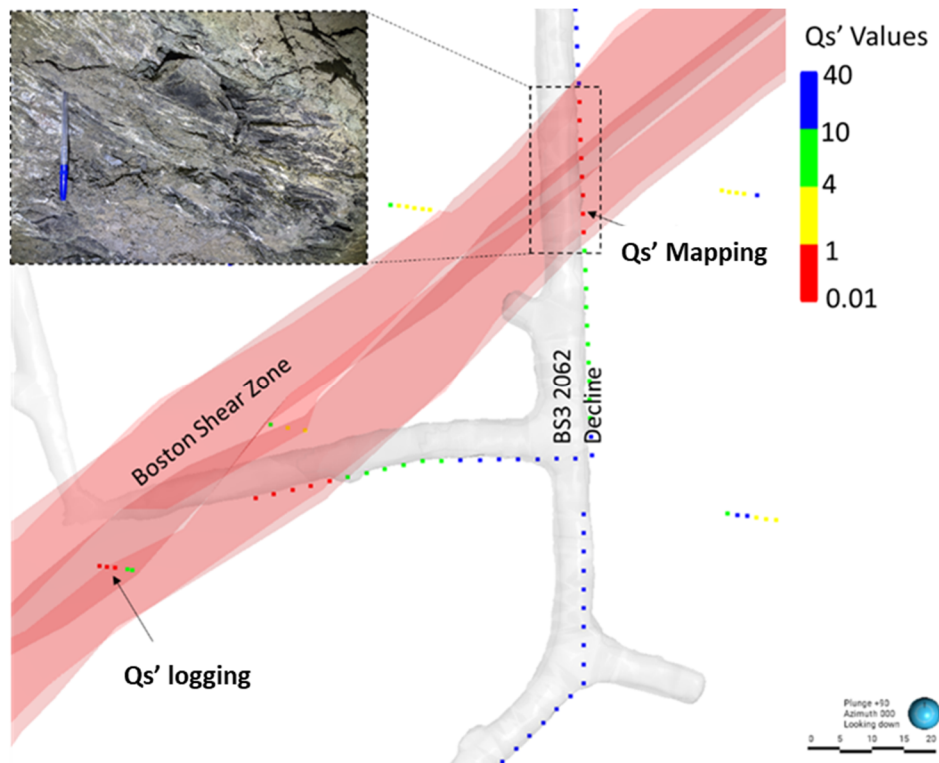


Figure 21 Plan view of Qs' logging of the Boston shear zone and Qs' mapping in development for the 2062 level

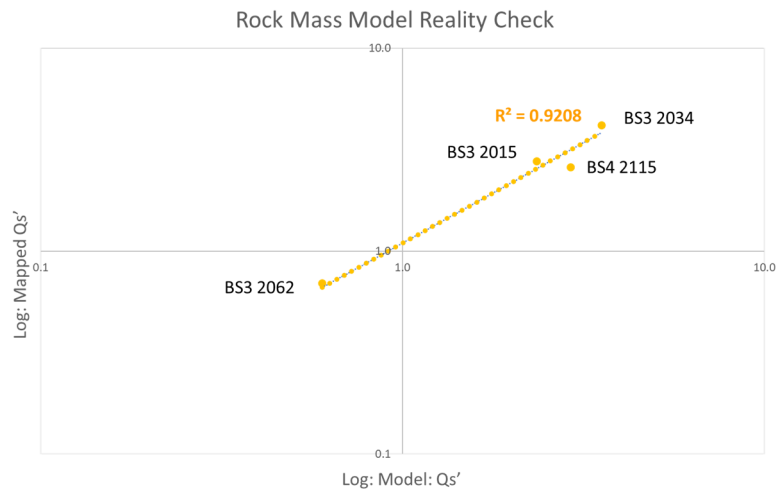


Figure 22 Validation performed for the rock mass model Qs' inverse distance squared weighted results in four levels for Boston Shaker

Due to orebody geometry, limited areas of loose rock, cement rockfill (CRF) and cement aggregate fill (CAF) are available for backfill. This means pillars must remain serviceable for the life of mine to mitigate the risks associated with migrating voids (caving) compromising infrastructure and airblast risk, while also facilitating an economic underground mine. Periodic drone flights by a specialist external contractor are completed across multiple historical levels to proactively monitor these risks and allow validation and refinement of pillar design assumptions used in the mine schedule.

The GMRI provides the ability to forecast declining extraction ratios at depth due to increased stress levels, which allows the business to proactively investigate alternative mining and backfill options many years in advance. The orebody is highly undulating, resulting in many different pillar orientations being used at a stope note and area note stage, aiming to keep the pillar perpendicular to that particular section of the ore zone. Pillar azimuth (dip direction) is a key component for average pillar stress levels, as some areas align to Sigma1 (higher average stress) and others are effectively shadowed to Sigma1 (lower average stress) (Figure 24).

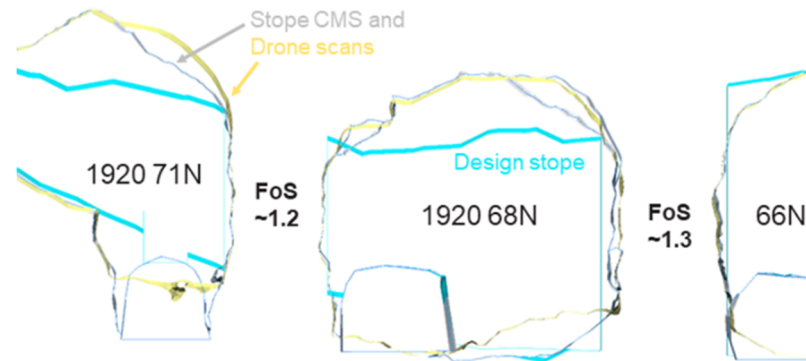


Figure 23 Estimated pillar stability based on modelled stresses, observed hour-glassing and width:height ratio for the BS3 1920 level

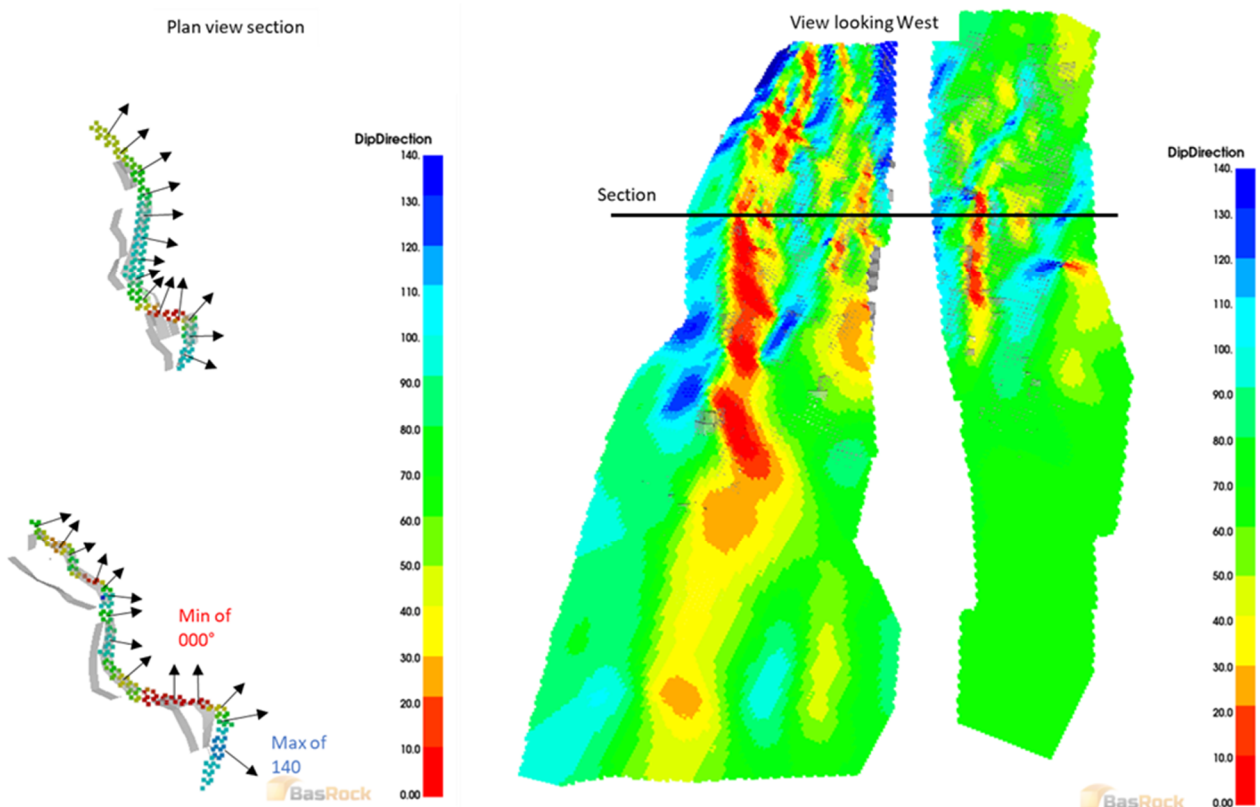


Figure 24 Pillar orientation coloured onto the hanging wall grid for a typical mining area, showing a high degree of orebody undulation

The voxel method in Map3D forecasts average pillar stresses for varying pillar orientations and mining depths for use in the GMRI (Figures 25 and 26). This average pillar stress is used with the UCS (calculated from Equotip measurements) to back-calculate a required W:H ratio and resulting rib pillar strike based on a FoS = 1.2 design curve interpreted from the empirical Lunder & Pakalnis (1991) pillar stability graph.

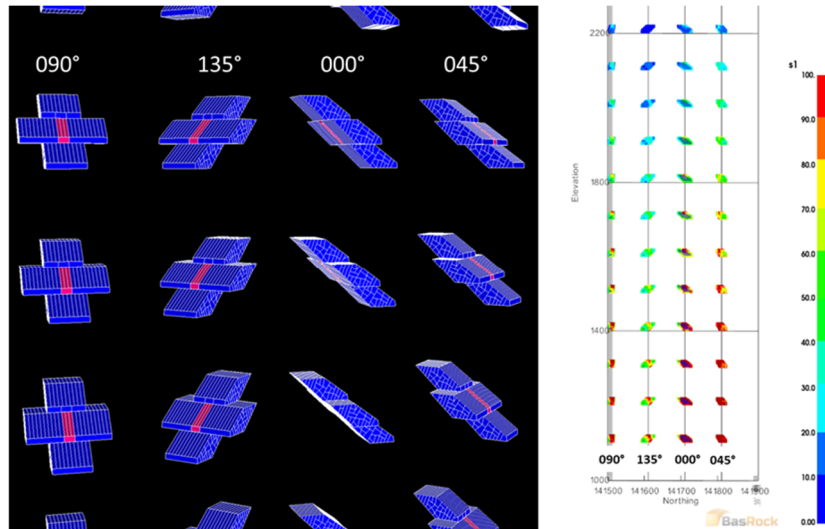


Figure 25 Pillar orientation modelling with depth using voxel method in Map3D

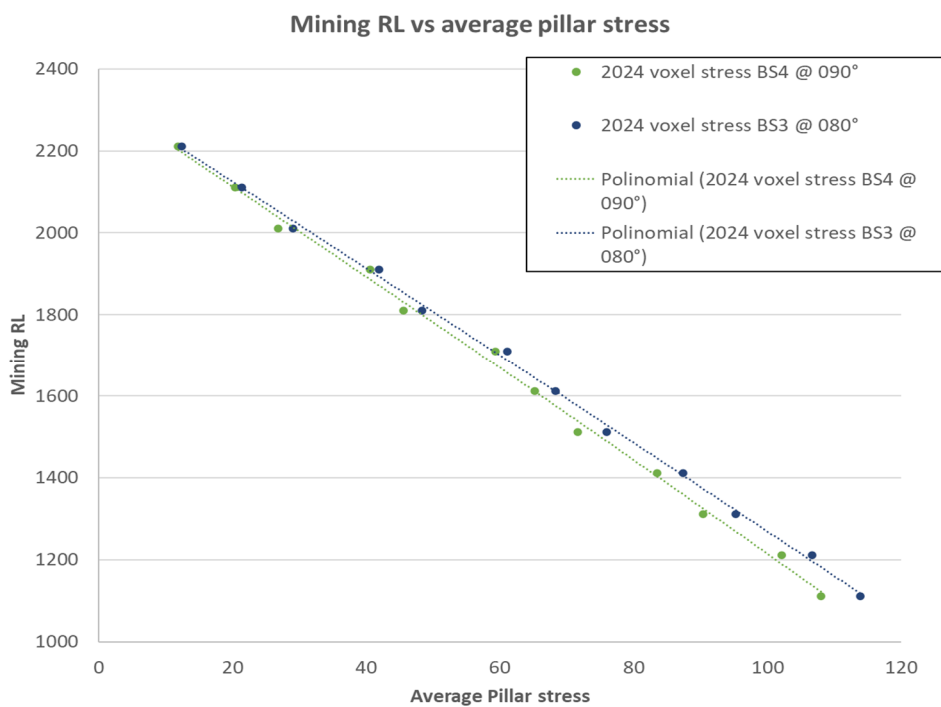


Figure 26 Average pillar stress at depth (for a 'typical' pillar orientation)

Practical limits for stoping and pillars at TGM were built into the site's GMRi based on the lessons learned over the last five years of stoping. These include HW hydraulic radius top cut at 7 m, rib pillar at 6 m minimum, pillar W:H bottom cut at 0.4, and a site-calibrated stoping ELOS design curve of 1.7 m (Fernandes et al. 2024). These practical limits build reliability into the site's GMRi and flow-on reliability into the various mine plan and schedule options. Localised opportunities for stoping beyond these limits are investigated as part of the stope note process.

The geotechnical team on site tracks stope overbreak through reconciliation each month, with a target level of ELOS accuracy between predicted (during stope note) and measured stope behaviour of ± 0.5 m (Figure 27). Some stope outliers exist in the dataset, allowing the geotechnical team opportunities to investigate why the stope overperformed or underperformed (dilution) and leading to refinement of predictions.

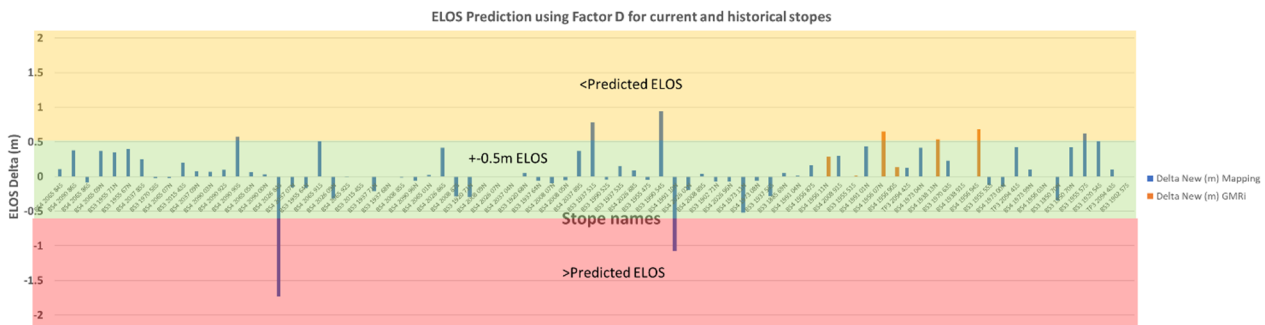


Figure 27 Variance between the predicted and actual equivalent linear overbreak sloughage in stope note assessment from monthly stope reconciliation

This level of confidence for predicted stope ELOS is particularly powerful in assessing mining areas in the long-term plan, many years ahead of time; significantly de-risking the medium- to long-term schedule for the business and building confidence.

4 Conclusion

Computational modelling has always been a time-consuming process, with the modelling work itself and the software processing time. Considering both components, overall timesaving is one of the main benefits of having an implicit and streamlined process.

By implementing this rock mass modelling methodology and framework, geotechnical inputs required for the business strategy and budgeting cycles are produced quicker and more consistently. Previously the mine used three separate Leapfrog projects that each had to be updated to encompass the entire underground life of mine. For each one of the projects, the data and geology had to be reviewed and manually imported into the software, with all analyses and estimations manually updated and cross-validated. The new combined model and semi-automated process is now updated in one single project, synced to the geological model that provides the model outputs for the three underground mines: Boston Shaker, Havana and Tropicana.

The processing time has halved since all repetitive steps in the previous methodology are now implicitly linked, streamlined and processed simultaneously. The RMM was previously updated quarterly. Now, after implementing the semi-automated process, the seamless model updates are carried out every time new data is available, or the geology model has been updated or refined.

The GMRI methodology was implemented at TGM during the underground Boston Shaker feasibility study in 2019 and has been under calibration since then to ensure strong confidence in predicting ER%. Based on the back-analysis completed over the last five years of stoping, drilling bias adjustments for rock quality designation and J_n are now automatically completed to ensure that geotechnical data from the drillcore matches underground mapping data.

The GMRI proves to be a reliable geotechnical tool to manage and highlight risks and opportunities in advance. The current reconciliation results presented demonstrate that the model accuracy relies on managing uncertainty levels and addressing all biases identified before updating the models for their next use. Another benefit is that the methodology employed by TGM is fit for purpose, as the semi-automated model also provides modellers with more time to perform validation checks across the process and thus increase reliability in driving underground mine design and optimising mine performance.

Acknowledgement

The authors would like to acknowledge AGA and TGM technical and managerial staff for allowing this material to be presented.

References

- Banff, C 2018, *Tropicana Equotip Correlation Update – BS Drill Program*, internal document for AngloGold Ashanti.
- Basson, FRP 2024, *GEM4D*, computer software, BasRock, Perth, <https://www.basrock.net/gem4d>
- Briggs, T 2023, 'AngloGold Ashanti at the 2023 Diggers and Dealers Conference', paper presented at Diggers and Dealers Forum, Kalgoorlie, 7–9 August.
- Clark, L & Pakalnis, R 1997, 'An empirical design approach for estimating unplanned dilution from open stope hanging walls and footwalls', *99th Annual AGM–CIM Conference*.
- Deswik 2024, *Deswik.Spatial*, computer software, <https://www.deswik.com/wp-content/uploads/2023/07/Deswik.Spatial-Brochure-UGM.pdf>
- Fernandes, S, Reardon, D & Cowan, M 2024, 'Stope design calibration at Boston Shaker underground mine for applications to bulk mining in a shallow dipping orebody', in H Schunnesson (ed.), *Proceedings of the 9th International Conference And Exhibition On Mass Mining (MassMin 2024)*.
- Hamman, ECF, du Plooy, DJ & Seery, JM 2017, 'Data management and geotechnical models', in J Wesseloo (ed.), *Deep Mining 2017: Proceedings of the Eighth International Conference on Deep and High Stress Mining*, Australian Centre for Geomechanics, Perth, pp. 461–487, https://doi.org/10.36487/ACG_rep/1704_33.2_Hamman
- Isaaks, EH & Srivastava, RM 1989, *An Introduction to Applied Geostatistics*, Oxford University Press, New York.
- Lunder, PJ & Pakalnis, R 1991, 'Determination of the strength of hard-rock mine pillars', *CIM Bulletin*, vol. 90, no. 1013, pp. 51–55.
- Mathews, K, Hoek, E, Wyllie, D & Stewart, S 1981, *Prediction of Stable Excavations for Mining at Depth Below 1000 Metres in Hard Rock*, DSS File No. 17SQ.23440-0-90210, Report to Canada Centre for Mining and Energy Technology (CANMET), Department of Energy and Resources, Ottawa.
- Norwegian Geotechnical Institute 2015, *Using the Q-system for Rock Mass Classification and Support Design*.
- Potvin, Y 1988, *Empirical Open Stope Design in Canada*, PhD thesis, The University of British Columbia, Vancouver.
- Reardon, D 2023, *Havana Underground Feasibility Study*, internal document for AngloGold Ashanti.
- Seequent 2024, *Leapfrog*, computer software, <https://www.seequent.com/products-solutions/leapfrog-geo>
- Wiles, T 2023, *Map3D*, computer software, Map3D International Ltd, <https://www.map3d.com>